Amino Acids (2011) 40:221–238
DOI 10.1007/s00726-010-0638-8

ORIGINAL ARTICLE

# Characterization, using comparative proteomics, of differentially expressed proteins in the hippocampus of the mesial temporal lobe of epileptic rats following treatment with valproate

**Liwen Wu · Jing Peng · Chaoping Wei · Gu Liu · Guoli Wang · Kongzhao Li · Fei Yin**

Received: 21 November 2009 / Accepted: 19 May 2010 / Published online: 4 June 2010


**Abstract** The objective of the study was to explore the pathogenesis of mesial temporal lobe epilepsy (MTLE) and the mechanism of valproate administration in the early stage of MTLE development. We performed a global comparative analysis and function classification of differentially expressed proteins using proteomics. MTLE models of developmental rats were induced by lithium-pilocarpine. Proteins in the hippocampus were separated by 2-DE technology. PDQuest software was used to analyze 2-DE images, and MALDI-TOF-MS was used to identify the differentially expressed proteins. Western blot was used to determine the differential expression levels of synapse-related proteins synapsin-1, dynamin-1 and neurogranin in both MTLE rat and human hippocampus. A total of 48 differentially expressed proteins were identified between spontaneous and non-spontaneous MTLE rats, while 41 proteins between MTLE rats and post valproate-treatment rats were identified. All of the proteins can be categorized into several groups by biological functions: synaptic and neurotransmitter release, cytoskeletal structure and dynamics, cell junctions, energy metabolism and mitochondrial function, molecular chaperones, signal regulation and others. Western blot results were similar to the changes noted in 2-DE. The differentially expressed proteins, especially the proteins related to synaptic and neurotransmitter release function, such as synapsin-1, dynamin-1 and neurogranin, are probably involved in the mechanism of MTLE and the pharmacological effect of valproate. These findings may provide important clues to elucidate the mechanism of chronic MTLE and to identify an optimum medication intervention time and new biomarkers for the development of pharmacological therapies targeted at epilepsy.

**Keywords** Mesial temporal lobe epilepsy · Hippocampus · Valproate · Proteomics · Mechanism

**Abbreviations**

| | |
|---|---|
| AEDs | Antiepileptic drugs |
| Cx50 | Gap junction channel protein connexin 50 |
| 2-DE | Two-dimensional polyacrylamide gel electrophoresis |
| F-actin | Actin filaments |
| HSPs | Heat shock proteins |
| IML | Inner molecular layer |
| MALDI-TOF-MS | Matrix-assisted laser desorption/ionization time-of-flight mass spectrometry |
| MAPKK1 | Dual specificity mitogen-activated protein kinase kinase 1 |
| MTLE | Mesial temporal lobe epilepsy |
| SE | Status epilepticus |
| SIR2-like | NAD-dependent deacetylase sirtuin-2 |
| TCP-1 | T-complex protein 1 |
| VPA | Valproate |

## Introduction

Epilepsy is a common and heterogeneous neurological disorder arising from biochemical and molecular events

L. Wu · J. Peng · C. Wei · G. Liu · G. Wang · K. Li · F. Yin (✉)
Department of Pediatrics, Xiangya Hospital, Central South University, Changsha 410008, Hunan, People's Republic of China
e-mail: yf3079@foxmail.com

that are yet to be fully understood. The pathogenesis and development of epilepsy and the response to antiepileptic drugs (AEDs) are varied, corresponding to different stages in the developing brain. In immature brains, there is enormous potential for growth and modification of the structure and function of the neurotransmitters and receptors related to epilepsy (Moshe 1993). Developmental changes from infancy to adulthood, plasticity and learning also contribute to the pathophysiology of epilepsy.

Mesial temporal lobe epilepsy (MTLE) is the most common epilepsy syndrome, with pharmacologically intractable partial-onset seizures. The pathological substrate of the syndrome is hippocampal sclerosis (HS) (Engel 1996). Therefore, to investigate the pathological characteristics of MTLE, most current studies focus on structural and functional changes in HS. Recent molecular research work on MTLE has focused on regeneration and synaptic plasticity (Timofeev et al. 2009), cytoskeletal changes (Wong 2008), cellular metabolism, protein synthesis (Sarac et al. 2009), neurotransmission, signal transduction (Kapur 2008), gliosis (Jabs et al. 2008) and ion channel changes (Graves 2006). Epileptic seizures can induce pathological processes of plasticity in the brain that tend to promote the generation of further seizures. Lopantsev (Lopantsev et al. 2009) reported that ictal epileptiform discharges could induce rapid plasticity at inhibitory and excitatory synapses in the hippocampus. A few seizure-like ictal episodes were sufficient to cause fast and lasting changes in the excitation/inhibition balance in hippocampal networks, which may contribute to early phases of progressive epileptogenesis. The synaptic-related protein dynamin-1 is required for synaptic vesicle endocytosis, and synapsin-1 is thought to mediate the interaction of synaptic vesicles with the presynaptic cytomatrix. Both dynamin-1 and synapsin-1 play a role in the regulation of the exo/endocytotic cycle of synaptic vesicles, and therefore of neurotransmitter release (McPherson et al. 1994).

Also, MTLE is the most common refractory form of epilepsy in adults, which remains a major clinical problem (Kwan and Brodie 2000). In a significant fraction of MTLE patients, complex partial seizures cannot be controlled by tolerable doses of AEDs. The most effective AEDs for MTLE, such as carbamazepine and phenytoin, do not adequately control seizures in adults when administered at doses that do not evoke intolerable side effects. In a select group, freedom from seizures can be attained by surgical resection of the epileptogenic zone. Therefore, not all of the patients can tolerate the operation and, in developing countries, surgical excision cannot be carried out thoroughly because of technical and economic reasons. So, further studies to explore new strategies and targets for pharmacological seizure controls are needed. In MTLE animal models, valproate (VPA) at a relatively high dose has been shown to achieve a complete remission of seizures (Leite and Cavalheiro 1995). VPA is a traditionally used AED with broad-spectrum effects, which has been investigated for the past four decades with demonstrated effects in a variety of models. One of the main targets of VPA is the processing actions in the GABAergic synapse through increasing GABA synthesis and hampering its metabolism by inhibiting several enzymes related to the tricarboxylic acid cycle and the GABA shunt, thereby modulating intracellular signaling pathways (Landmark 2007). Actually, VPA inhibits cerebral energy metabolism by enzyme inhibition, which may modulate neuronal excitability. Therefore, the effect of VPA on voltage-gated sodium channels, in addition to potassium and calcium channels, is no longer regarded as an important, clinically relevant mechanism of action (Johannessen et al. 2001).

In our previous experiment (Wu et al. 2009), we found that early administration of VPA at or before the onset of epilepsy could achieve seizure freedom in rats where MTLE was induced by lithium-pilocarpine on postnatal day 25. This suggests that we could achieve a pharmacological control for refractory MTLE by administering AEDs at an early stage. As mentioned above, recent studies on the pathogenesis of MTLE have focused on synaptic plasticity, neurotransmission, cellular metabolism and ion channel changes. The main therapeutic targets of VPA are the GABAergic synapse, energy metabolism and ion channels. We propose a novel approach: investigating the mechanism of VPA on MTLE at an early stage to explore new targets for pharmacological treatment.

Biomarker searching and protein profiling in MTLE have been carried out in recent years using proteomic methods (Liu et al. 2008; Greene et al. 2007). The recent application of two-dimensional electrophoresis (2-DE) coupled with matrix-assisted laser desorption/ionization time-of-flight mass spectrometry (MALDI-TOF-MS) in the study of VPA-treated and untreated MTLE rats allows the characterization of global alterations in protein expression due to pharmacological intervention. A series of differentially expressed proteins have been found and partials have been validated by Western blot. Furthermore, we have confirmed the expression levels of synapse-related proteins, synapsin-1, dynamin-1, and neurogranin, in MTLE human patient hippocampus by collecting postoperative hippocampus tissue.

This study aims to identify biomarkers related to the pathogenesis of MTLE via protein profiles in the pilocarpine rat models and to explore VPA-related protein changes. We will evaluate the clinicopathological characteristics of this disease by studying the expression of the target proteins, enabling us to better understand the mechanisms of MTLE and the impact of VPA's administration in the early stage of MTLE development.

## Materials and methods

### Materials and chemicals

The 2-DE equipment, ImageScanner, ImageMaster 2D Elite 4.01 analysis software, protein assay kit and supply materials (Immobiline DryStrips pH 3–10L, 24 cm) were purchased from Amersham Biosciences. Chemicals were mainly obtained from Amresco (Solon, OH, USA). Pilocarpine, valproate and trypsin were obtained from Sigma (St. Louis, USA). All other chemicals were of analytical reagent grade. PVDF blotting membranes, ECL and Hyperfilm, and rabbit polyclonal antibody against neurogranin, dynamin-1 and synapsin-1 were from Abcam, Inc. The Applied Biosystem Voyager-DETM STR Biospectrometry™ Workstation System 4307 MALDI-TOF MS was purchased from Applied Biosystems.

### MTLE patients and controls

Specimens were obtained at surgery from five patients, with drug-resistant MTLE with typical imaging features and pathological confirmation of hippocampal sclerosis, who had unilateral selective amygdalohippocampectomy. The decision for surgery was based on convergent evidence of clinical and EEG recordings during prolonged video-EEG monitoring and high-resolution magnetic resonance imaging indicating mesial temporal lobe seizure onset. Surgical specimens were examined by routine pathology. As control tissue, five normal hippocampal samples were obtained at autopsy from patients (postmortem delay: maximum 24 h) with no history of brain disease. Clinical information on MTLE patients and controls are presented in Table 1. This study was approved by the Institutional Ethics Committee of Central South University and informed consents were obtained from all patients prior to analysis.

### Animals

In this study, 25-day-old Sprague–Dawley rats of either sex (obtained from the Experimental Animal Center, Central South University) were used. Following arrival, animals were maintained in a room with a controlled light–dark cycle (lights on from 07:00 to 19:00 h) and a constant temperature (20 ± 2°C). They were allowed to adapt to laboratory conditions for at least 1 week before starting the experiments. All procedures were approved by the Institutional Animal Care and Use Committee of Central South University.

### Epilepsy induction and VPA treatment

On postnatal day 25, the rats ($n = 50$) were injected with lithium chloride (3 mEq/kg, i.p.) 18–20 h before pilocarpine treatment. Methylscopolamine (1 mg/kg, i.p.), a muscarinic antagonist that does not cross the blood–brain barrier was administered 15 min prior to pilocarpine treatment to reduce the peripheral effects of the convulsant and thus enhance survival. Pilocarpine hydrochloride

**Table 1** Clinical characterization of MTLE patients and controls

| ID | Sex | Age (years) | Duration of epilepsy (years) | Side of hippocampus sample | Antiepileptic drugs (AED) |
|---|---|---|---|---|---|
| Patients with MTLE | | | | | |
| E1 | M | 9 | 0.6 | L | CBZ, LAM |
| E2 | F | 20 | 20 | R | VPA, CBZ, TOP |
| E3 | M | 20 | 6 | R | CBZ, VPA, LEV |
| E4 | M | 25 | 3 | R | CBZ, VPA, LAM |
| E5 | F | 27 | 13 | L | VPA, CBZ, TOP |
| ID | Sex | Age (years) | Post-mortem interval (h) | Side of hippocampus sample | Causes of death |
| Controls | | | | | |
| C1 | M | 28 | 23 | R | Hodgkin's disease |
| C2 | M | 19 | 18 | L | Chronic myelocytic leukemia |
| C3 | F | 8 | 15 | R | Pneumorrhagia |
| C4 | M | 14 | 20 | R | Acute pancreatitis |
| C5 | F | 23 | 15 | L | Cardiormyopathy |

*CBZ* carbamazepine, *LAM* lamotrigine, *LEV* levetiracetam, *VPA* valproate, *TOP* topiramate, *R* right, *L* left

*C1–C5* represented five patients without brain disease, *E1–E5* represented five patients with MTLE

(30 mg/kg, i.p.) was then injected to induce status epilepticus (SE). Diazepam (10 mg/kg, i.p.) was administered 90 min after the onset of SE to terminate the seizure. The rats not up to SE ($n = 5$) were removed in the experiment. Following pilocarpine treatment, the rats were video-monitored for 8 weeks. As we observed that the spontaneous seizures usually occurred around 3 weeks after SE, VPA (200 mg/kg, i.p.) was given three times per day at 8:00, 11:00 and 14:00 h for 2 weeks beginning at 3 weeks after SE. Control rats received all treatments with the exception of saline instead of VPA. At 8 weeks after pilocarpine administration, all the rats could be divided into three groups: the VPA-treated group ($n = 13$, the pilocarpine-induced rats who received VPA treatment); the untreated rats could be divided into two groups, the epilepsy group ($n = 14$, the pilocarpine-induced rats who developed spontaneous seizure) and the non-epilepsy group ($n = 18$, the pilocarpine-induced rats who did not develop spontaneous seizure).

### Morphological observation

Three groups of animals subjected to pilocarpine-induced SE were perfused at the time point of 8 weeks after pilocarpine-induced SE and processed for nissl and neo-Timm staining. Rats (two rats of each group) were deeply anesthetized with thionembutal and sequentially perfused through the heart with (1) 25 ml of Millonig's buffer; (2) 50 ml of 0.1% sodium sulfide fixative in Millonig's buffer; (3) 100 ml of 3% glutaraldehyde; (4) 200 ml of 0.1% sodium sulfide fixative in Millonig's buffer. Their brains were removed and immersed in 30% sucrose overnight. Frozen coronal sections were then processed for nissl staining (8 μm) and neo-Timm staining (30 μm).

Nissl staining was applied to observe the extent of neurons loss. Cresyl violet was used as the nissl stain substance. Timm staining was used to label the zinc-rich axon terminals of granule cells according to a modified protocol (Babb et al. 1991). The processing solutions consisted of 240 ml of 50% gum arabic with 10.25 g of citric acid, 9.45 g sodium citrate in 30 ml of $ddH_2O$, 3.73 g hydroquinone in 60 ml of $ddH_2O$ and 2 ml solution of 0.51 g silver nitrate in 3 ml $ddH_2O$. The slides were processed in the processing solutions for 40–50 min, washed in distilled water twice for 5 min, dehydrated through alcohol to xylene and coverslipped with neutral balsam. The intensity of sprouting in the inner molecular layer (IML) of the hippocampus was used to evaluate the abnormal sprouting of moss fibers, which has been described in human mesial temporal sclerosis (Babb et al. 1991; Mathern et al. 1997) as well as in several animal models of temporal lobe epilepsy (Hamani et al. 2005; Williams et al. 2004).

### Sample preparation for 2-DE

The rest of the rats in the three groups were killed under deep flurothyl anesthesia 8 weeks after pilocarpine-induced SE. The brains were removed from the skull and the hippocampal tissues were rapidly dissected and immediately frozen on dry ice and stored in liquid nitrogen. A total of 30–80 mg of hippocampus was ground to powder in liquid nitrogen, dissolved in 400 ml lysis buffer (7 mol/l urea, 2 mol/l thiourea, 2% NP-40, 1% Triton X-100, 100 mmol/l DTT, 5 mmol/l PMSF, 4% CHAPS, 0.5 mmol/l EDTA, 40 mmol/LTris, 2% pharmalyte, 1 mg/ml DNase I, and 0.25 mg/ml RNase A), vortexed and incubated (4°C, 60 min). The mixture was centrifuged (12 000 rpm/min, 60 min, 4°C). The obtained supernatants containing proteins were then precipitated with acetone (1:4, overnight, −20°C, followed by centrifugation at 12,000*g*, 10 min, at 4°C) for deionization. After removing residual acetone by air-drying, the protein pellets were re-dissolved with lysis buffer. After being centrifuged (12,000 rpm/min, 10 min, 4°C) again, the supernatant was the total protein solution. The concentration of the total proteins was determined by 2D-Quant Kit. Each sample was prepared individually. Eight samples of each group were chosen randomly and pooled with isoconcentration to minimize potential inter-individual differences before 2-DE. All of the proteins were stored at −80°C.

### 2-DE

The pooled samples of the three groups (1 mg for preparative gels) were diluted in rehydration buffer (7 M urea, 2 M thiourea, 4% w/v CHAPS, 40 mM Tris base, 65 mM DTT, 0.5%v/v ampholyte pH 3–10 with a trace of Bromophenol Blue) to give a final volume of 450 μl and applied on immobilized 24 cm pH 3–10 linear gradient strips by in-gel passive rehydration for 13 h. IEF was run subsequently for 1 h at 500 V, 1 h at 1,000 V, 1 h at 5,000 V and 8.5 h at 8,000 V to reach a total of 68 kVh. Following IEF separation, the gel strips were equilibrated for 15 min in a solution [6 mol/l urea, 2% SDS, 30% glycerol, 50 mmol/l Tris–HCl (pH 8.8), and 1% DTT] and then for an additional 15 min in the same solution, except that DTT was replaced by 2.5% iodoacetamide. After equilibration, SDS-PAGE was done on the Ettan DALT II system. After electrophoresis, the gels were stained with colloidal Coomassie blue G-250 and scanned by an Imagescanner. PDQuest 7.3.1 software was employed for the image analysis, including background abstraction, spot intensity calibration, spot detection and matching. The intensity of each spot was quantified by a calculation of spot volume after normalization of the gel image. Each sample was performed in triplicate, and a paired Student's *t* test was applied to compare the spot relative volume

(% volume, the ratio of the volume of a spot to the volume of the spots from the entire gel) corresponding to each target spot across the gels.

### In-gel protein digestion and MALDI-TOF-MS

After the image analysis, the significantly differential spots were chosen for MALDI-TOF-MS analysis. The spots were excised from the gels and destained at room temperature in 50 mM $NH_4HCO_3$ buffer for 1–2 h and dehydrated with 100% ACN. Then the vacuum centrifugation-dried gel pieces were digested overnight at 37°C in a solution comprising 40 mmol/l $NH_4HCO_3$, 9% ACN and 20 μg/ml trypsin TPCK-trypsin. The tryptic peptide mixture was extracted and purified using a Millipore ZIP-TIP$^{TM}$ C18 column. The purified tryptic peptide mixture was mixed with CHCA matrix solution and vortexed lightly. A volume (1 μl) of the mixture containing CHCA matrix was loaded onto a stainless steel plate and air-dried. The samples were analyzed with an Applied Biosystems Voyager System 4307 MALDI-TOF Mass Spectrometer (ABI). The parameters were set up as follows: positive ion-reflector mode, accelerating voltage of 20 kV, grid voltage of 64.5%, mirror voltage ratio of 1.12, $N_2$ laser wavelength of 337 nm, pulse width of 3 ns, the number of laser shots 50, acquisition mass range of 1,000–3,000 Da, delay of 100 ns and vacuum degree of $4 \times 10^7$ Torr. A trypsin-fragment peak served as an internal standard for mass calibration. A list of the corrected mass peaks was the peptide mass fingerprint.

### Protein identification and database analysis

Protein identification using PMF was performed by MASCOT Distiller (http://www.matrixscience.com/, Matrix Science Ltd, UK) against the Swiss-Prot protein database. The search parameters were set up as follows: the taxonomy was Rattus, the enzyme was trypsin, the number of missed cleavage sites was allowed to go up to 1, the fixed modification was carbamidomethylation, the variable modification was oxidation, the peptide tolerance was 50 ppm, the mass value was $MH^+$, searching range was pI value ±0.5 pH unit and the experimental mass range (Mr) was ±20%. The criteria for positive identification of proteins were set as follows: (1) the MS match consisted of a minimum of five peptides; (2) the matched peptides covered at least 20% of the whole protein sequence; (3) the MASCOT score of a protein match was higher than 51 ($p < 0.05$).

### Validation by Western blot

The individual protein sample in each group was chosen randomly for Western blot. In total, 30 μg of total protein was run on a 10% sodium dodecyl sulfate-polyacrylamide (SDS-polyacrylamide) gel, and the PVDF membranes were incubated overnight at 4°C with polyclonal antibodies against neurogranin, synapsin-1 and dynamin-1 (Abcam, Inc) at 1:1,000 dilutions, respectively. They were subsequently incubated with HRP-conjugated sheep anti-rabbit IgG (Amersham Biosciences) at 1:2,000 dilutions. $\beta$-actin was used as loading control. The reactions were visualized using an enhanced chemiluminescence (ECL) detection system. Signals on the blots were visualized by autography. The film signals were digitally scanned and then quantified using FluorChem software. The experiments were performed in triplicate.

### Statistics

All experimental data were presented as mean ± SD and analyzed by Student's $t$ test using SPSS software (version 13.0, SPSS). Statistical significance was defined as $p \leq 0.05$.

## Results

### Animal model

For each pilocarpine-treated animal, clinical signs of seizure activity were observed. All rats exhibited a well-defined pattern of behavior after pilocarpine treatment, such as akinesia, ataxic lurching, tremor, head bobbing, masticatory automatisms with myoclonus of facial muscles and wet dog shakes at onset. Then 90% of the rats ($n = 45$) progressed to SE with bilateral limbs clonus, rearing and falling around 15–35 min after an injection of pilocarpine.

Spontaneous seizures usually occurred 3 weeks after pilocarpine administration. As we observed, spontaneous seizures were generally characterized by a focal onset (immobility, mechanical mutation, mouth clonus, forelimb clonus), occasionally culminating into a generalized convulsive stage lasting about 30 s to 1.5 min, one to several times per day. These behavioral changes were quite consistent with the features of human MTLE. As much as 60% ($n = 27$) of the pilocarpine-processed SE rats developed spontaneous seizure. The 18 remaining rats, considered as the non-epilepsy group ($n = 18$), behaved like normal rats with no spontaneous seizures. Among the rats with spontaneous seizures, 13 were treated with VPA and were regarded as the VPA-treated group ($n = 13$). Following 2 weeks of administration of VPA, the rats were video-monitored for a 3-week period. A complete remission of seizures was observed in the rats of the VPA-treated group, accompanied with side effects of lassitude and less activity. The remaining 14 rats which showed recurrent seizures were considered as the epilepsy group ($n = 14$).

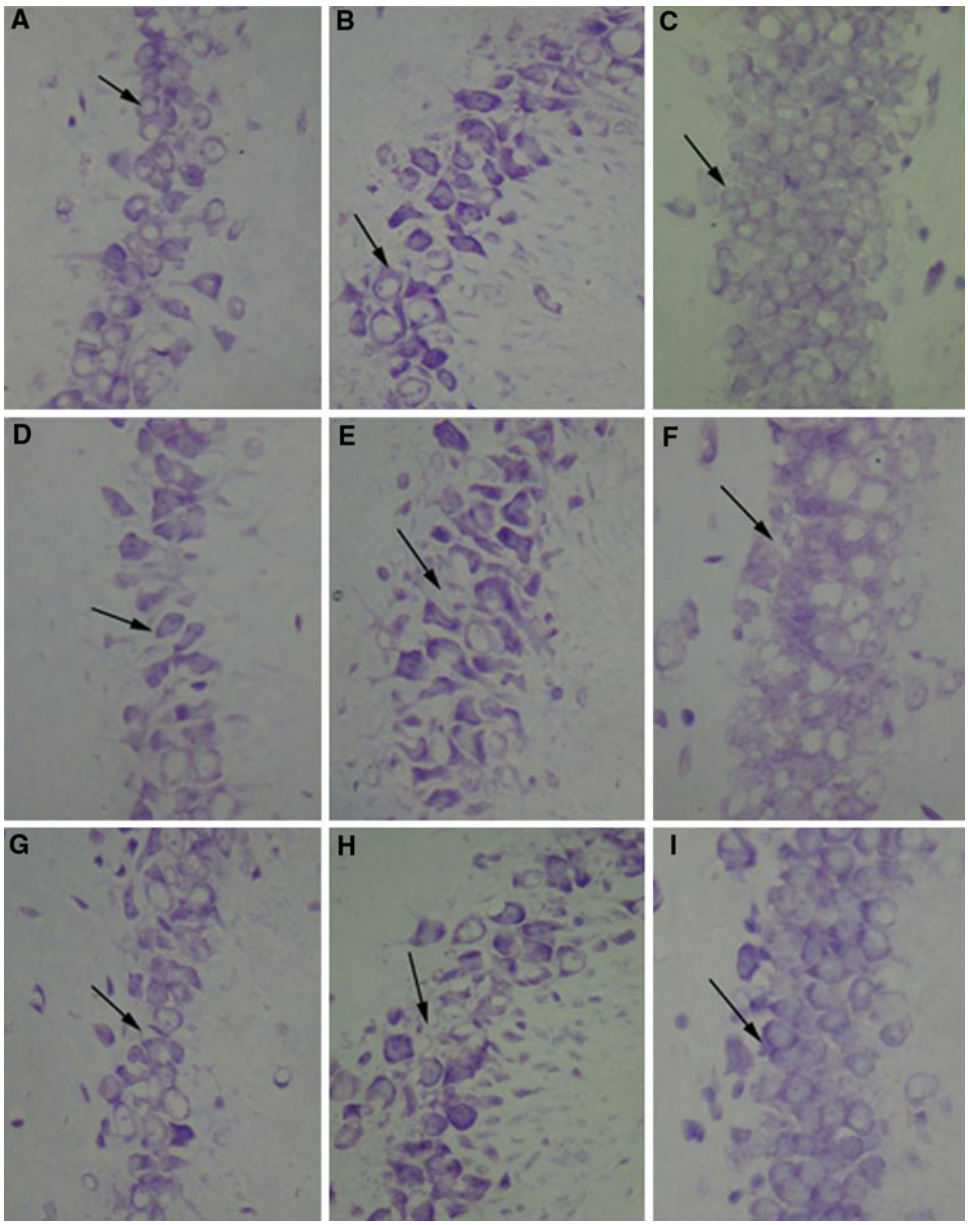


**Fig. 1** Nissl staining of hippocampus (1:400) Nissl-stained sections reveal many neurons in the dentate gyrus (**c**, **f**, **i**), CA1 region (**a**, **d**, **g**), CA3 region (**b**, **e**, **h**) of the VPA-treated group (**g**, **h**, **i**) and non-epilepsy group (**a**, **b**, **c**); inversely, the neuron numbers were significantly decreased in the corresponding areas in the epilepsy group (**d**, **e**, **f**), instead of a large amount of reactive neurons, plasticity and gliosis. The epilepsy group was with more severe neuron loss compared with the non-epilepsy group, which was improved after VPA treatment

## Morphological observation

Nissl-stained sections (Fig. 1) revealed many neurons in the dentate gyrus, CA1 region and CA3 regions of the VPA-treated group and non-epilepsy group; inversely, the neuron numbers in the corresponding areas were significantly decreased in the epilepsy group, which exhibited a large amount of reactive neurons plasticity and gliosis. Timm-stained sections (Fig. 2) revealed a relatively normal pattern of staining in the VPA-treated group and non-epilepsy group. However, aberrant stainings in the dentate gyrus and IML of the epilepsy group were observed. The results of nissl and Timm stains showed that the morphological observations in VPA-treated rat hippocampus relatively approached that of the non-epilepsy rats compared with the epilepsy rats. All of these observations suggested that early administration of VPA had neuroprotective effects in our MTLE rat models and could prevent neurons loss and abnormal mossy fiber from sprouting.

## Comparative proteomic analysis

There were three 2-DE maps of each group obtained in this study. On comparing the 2-DE maps of the VPA-treated group, epilepsy group and non-epilepsy group, each displayed about $950 \pm 40$ spots, with an average matching rate of 89.7, 88.1 and 90.2%. Three representative 2-DE maps from each group are shown in Fig. 3. The 2-DE

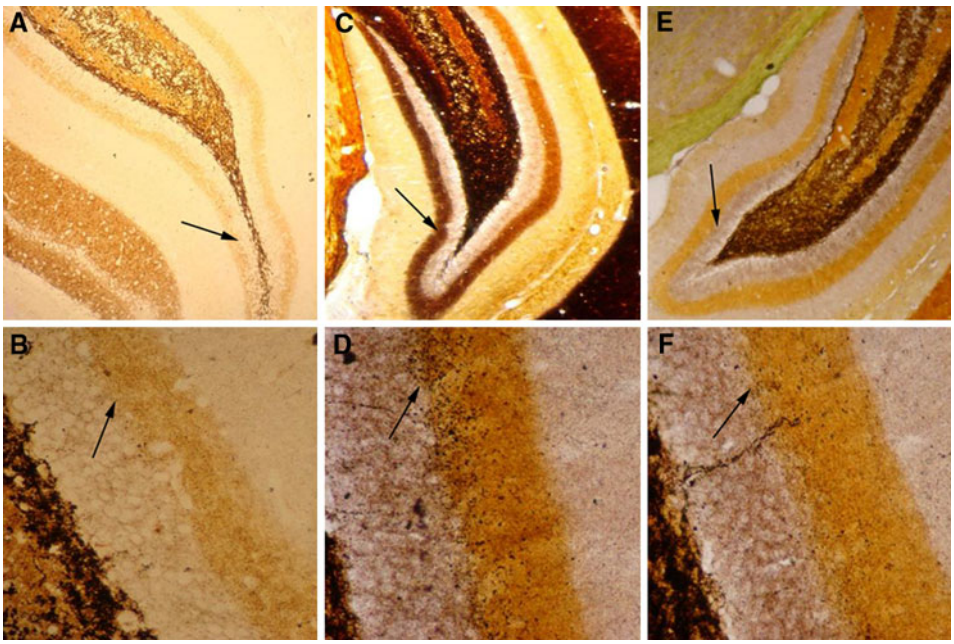


**Fig. 2** Timm staining of hippocampus **a**, **c** and **e**: The dentate gyrus (1:100); **b**, **d** and **f**: IML (1:200). Timm-stained sections reveal a normal and relatively normal pattern of staining in the non-epilepsy group (**a** and **b**) and VPA-treated group (**e** and **f**), while aberrant staining is shown in the IML of the epilepsy group (**c** and **d**). Estimated proportion of granule cell layer plus molecular layer was Timm positive: 3% (non-epilepsy group, **a** and **b**), 37% (epilepsy group, **c** and **d**) and 5% (VPA-treated group, **e** and **f**). The epilepsy group with more severe mossy fiber sprouting showed spontaneous bursts of dentate gyrus population spikes and after discharges compared with the non-epilepsy group, which was improved after VPA administration

patterns of the three groups were compared by automatic and manual matching, and the spots with differential expression over twofolds were regarded as differential expression protein spots. When the VPA-treated group was compared with the epilepsy group, 41 differential expression protein spots were identified and are marked with arrows in Fig. 3. Their details are shown in Table 2, including 14 spots up-regulated and 2 expressed only in the VPA-treated group, and 18 spots up-regulated and 7 spots expressed only in the epilepsy group. Likewise, comparing the epilepsy group and non-epilepsy group, 48 differential expression protein spots were identified and are marked with arrows in Fig. 3. Their details are shown in Table 3, including 17 spots up-regulated and 6 expressed only in the epilepsy group, and 23 spots up-regulated and 2 spots expressed only in the non-epilepsy group. Partial differential expression protein spots are shown in Fig. 4. Among the MALDI-TOF-MS identified proteins, 17 spots always up-regulated in the epilepsy group, regardless of whether the group was compared with the non-epilepsy or VPA-treated groups. Those proteins are shown in Table 4 and were likely involved in the pathogenesis of MTLE. Also, ten spots down-regulated in the epilepsy group compared with the non-epilepsy group, and up-regulated over twofolds after VPA administration. These proteins are probably related to the protective effects of VPA and are shown in Table 4.

### Validation by Western blot

The expression levels of the differentially expressed proteins, neurogranin, synapsin-1 and dynamin-1, were further confirmed using Western blot analysis (Fig. 5). We observed that dynamin-1 was remarkably down-regulated in the epilepsy group compared with the VPA-treated and non-epilepsy groups (both $p < 0.01$); similar changes were observed with synapsin-1 (both $p < 0.01$). Conversely, the protein expression of neurogranin increased significantly in the VPA-treated group (both $p < 0.01$). Hence, the results of Western blot analysis of these three proteins confirmed the reliability of the proteomic analysis.

The expression levels of neurogranin, synapsin-1 and dynamin-1 in the hippocampus of controls and patients with MTLE were consistent with the proteomic analysis results of the MTLE rat models, shown in Fig. 6. The protein expression of neurogranin increased significantly in MTLE patients ($p < 0.01$), while expression levels of synapsin-1 and dynamin-1 remarkably decreased in MTLE patients compared with controls (both $p < 0.01$).

## Discussion

To date, the mechanism of MTLE has been associated with impairment of the hippocampus induced by various

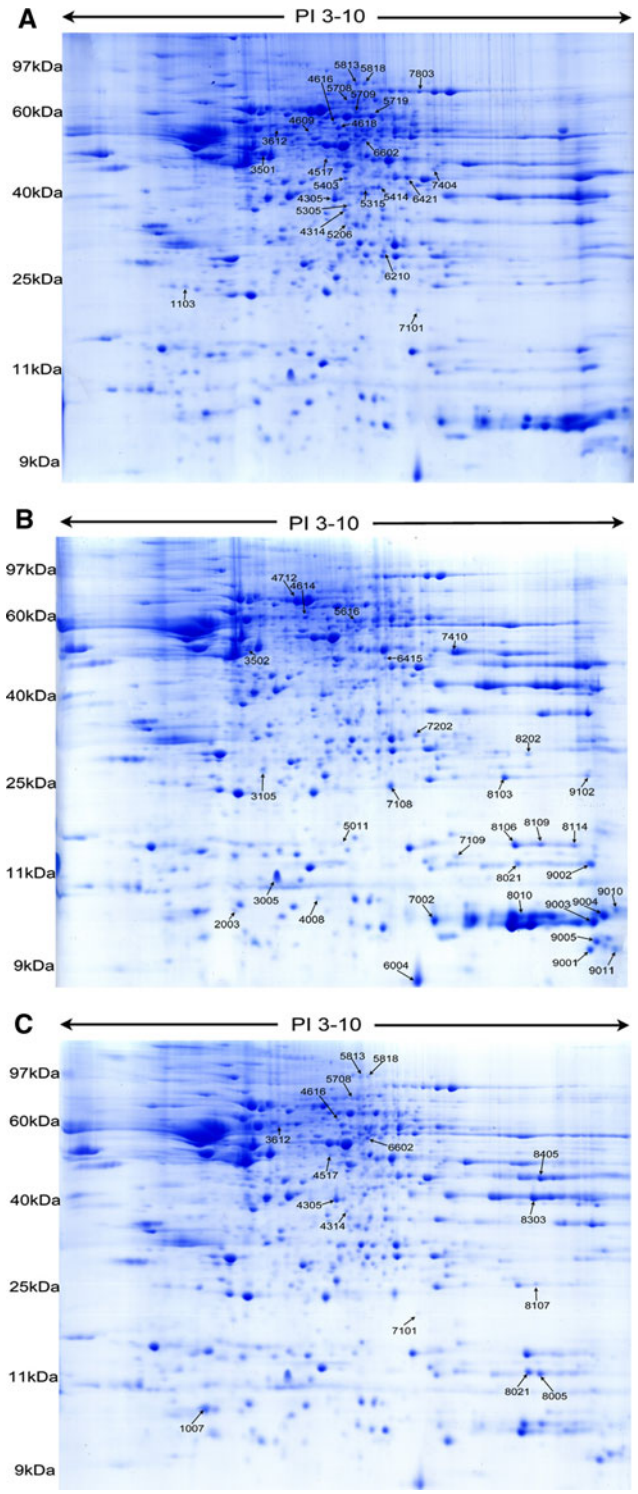


**Fig. 3** Representative 2-DE gel images of hippocampal protein extracts from rats of the non-epilepsy group (**a**), epilepsy group (**b**) and the VPA-treated group (**c**). 2-DE was performed in an immobilized pI 3–10 linear gradient strip, followed by second-dimensional separation on 12.5% gradient polyacrylamide gels, and the separated proteins were detected by colloidal Coomassie blue staining. Numbered differential protein spots were identified using MALDI-TOF-MS. Detailed information on these proteins is listed in Tables 2 and 3

damages (injury, convulsion or febrile seizure) in the early lifetime (Muramatsu et al. 2008). However, there are many kindling animal MTLE models where disease is induced by the application of an excitotoxic compound (kainic acid, pilocarpine) based on this mechanism (Gluck et al. 2000; Danzer et al. 2010). These animal models appear to be particularly helpful in studying the molecular mechanisms of MTLE and the development of pharmacological properties. As the MTLE in adults is difficult to control with AEDs (Kwan and Brodie 2000), and the pathogenesis and response to AEDs are varied in the immature brain (Moshe 1993), we hypothesize that it may be relatively easier to cure MTLE by using AEDs at an early stage before any formation of chronic lesions.

In this study, we used VPA in MTLE rat models at or before the spontaneous seizures occurred. We found that the VPA-treated rats obtained complete remission. Meanwhile, spontaneous seizures occurred frequently in parts of the rats of the non-treatment epilepsy group. Correspondingly, the Nissl and Timm staining results supported the notion that VPA had neuroprotective effects in our MTLE rat models, preventing abnormal mossy fiber sprouting and reducing neuron loss and degeneration. These findings suggest that we can alter the pathological changes that occur in MTLE rats by pharmacological treatment in the early development of MTLE and the changes in VPA-treated rats contrast with the pathological changes observed in the untreated MTLE rats, which were clinically intractable. This observation deserves further exploration to identify an optimum medication intervention time for the development of pharmacological therapies targeted at epilepsy.

A number of aspects of epilepsy are poorly understood, including its signaling mechanisms and its complex protein networks. However, technical developments in the field of proteomics are poised to generate advances in our understanding of protein expression, function and organization in signaling processes and regulatory networks, thus providing deeper insight into how cellular protein networks are regulated in the epileptic hippocampus under pathological conditions. The hippocampal protein expression profiles represent the functional status of MTLE. To study the pathogenesis of MTLE and to explore the mechanism of VPA on MTLE at the onset, this study performed a global proteomic analysis on the hippocampus of spontaneous seizure rats, non-spontaneous seizure rats and VPA-treated rats. The differentially expressed proteins we obtained can be categorized into several main groups by biological functions: synaptic and neurotransmitter release function, cytoskeletal structure and dynamics, energy metabolism and mitochondrial function, molecular chaperones, signal regulation and others. Differences between the expression

**Table 2** Identification of the differentially expressed proteins in rat hippocampus of the VPA-treated group compared with the epilepsy group by MALDI-TOF–MS

| Spots number | Primary accession number | Protein ID | Protein name | Score | Peptides matched | Sequence coverage (%) | Theoretical Mr/PI | Expected | Fold change |
|---|---|---|---|---|---|---|---|---|---|
| Up-regulated proteins in the epilepsy group | | | | | | | | | |
| 3005 | Q04940 | NEUG_RAT | Neurogranin | 82 | 5 | 43 | 7,720/6.54 | 4e-05 | 2 |
| 3105 | P04639 | APOA1_RAT | Apolipoprotein A-I | 113 | 10 | 54 | 30,043/5.52 | 3.6e-08 | 6.25 |
| 4008 | P02767 | TTHY_RAT | Transthyretin | 55 | 6 | 39 | 15,824/5.77 | 0.024 | 2.7 |
| 4614 | P11598 | PDIA3_RAT | Protein disulfide-isomerase A3 | 246 | 26 | 50 | 57,044/5.88 | 1.8e-21 | 5.56 |
| 8010 | P07335 | KCRB_RAT | Creatine kinase B-type | 58 | 7 | 15 | 42,983/5.39 | 0.011 | [a] |
| 8114 | P45592 | COF1_RAT | Cofilin-1 | 82 | 10 | 67 | 18,749/8.22 | 5.1e-05 | 2.94 |
| 8109 | P45592 | COF1_RAT | Cofilin-1 | 105 | 12 | 72 | 18,749/8.22 | 2.3e-07 | 2.94 |
| 7002 | P11517 | HBB2_RAT | Hemoglobin subunit beta-2 | 119 | 14 | 82 | 15,953/6.81 | 8.6e-08 | 6.25 |
| 6004 | P62989 | UBIQ_RAT | Ubiquitin | 100 | 9 | 77 | 8,560/6.56 | 7.6e-07 | 6.25 |
| 9011 | P56391 | CX6B1_MOUSE | Cytochrome c oxidase subunit VIb isoform 1 | 100 | 6 | 63 | 10,293/8.96 | 6.9e-06 | [a] |
| 4712 | P02770 | ALBU_RAT | Serum albumin | 184 | 29 | 52 | 62,638/5.95 | 2.8e-15 | 2.33 |
| 6415 | P43165 | CAH5A_RAT | Carbonic anhydrase 5A, mitochondrial | 52 | 5 | 23 | 34,477/8.48 | 0.044 | 3.85 |
| 7410 | P30275 | KCRU_MOUSE | Creatine kinase, ubiquitous mitochondrial | 187 | 25 | 58 | 47,373/8.39 | 1.4e-15 | 2 |
| 7202 | P27139 | CAH2_RAT | Carbonic anhydrase 2 | 105 | 6 | 35 | 29,267/6.89 | 2.3e-07 | 4.55 |
| 7108 | P39069 | KAD1_RAT | Adenylate kinase isoenzyme 1 | 164 | 14 | 68 | 21,684/7.66 | 2.8e-13 | 2.31 |
| 7109 | Q7M767 | UB2V2_RAT | Ubiquitin-conjugating enzyme E2 variant 2 | 66 | 6 | 45 | 16,399/7.79 | 0.0017 | 5.5 |
| 8202 | P63039 | CH60_RAT | 60 kDa heat shock protein, mitochondrial | 52 | 5 | 14 | 61,088/5.91 | 0.045 | [a] |
| 9102 | Q63716 | PRDX1_RAT | Peroxiredoxin-1 | 117 | 14 | 48 | 22,323/8.27 | 1.4e-08 | [a] |
| 5011 | P45592 | COF1_RAT | Cofilin-1 | 64 | 5 | 45 | 18,749/8.22 | 0.0029 | [a] |
| 9002 | P10111 | PPIA_RAT | Peptidyl-prolyl *cis–trans* isomerase A | 131 | 11 | 68 | 18,091/8.34 | 5.7e-10 | [a] |
| 9003 | P01946 | HBA_RAT | Hemoglobin subunit alpha-1/2 | 109 | 6 | 50 | 15,490/7.82 | 9e-08 | 110.59 |
| 9005 | P26772 | CH10_RAT | 10 kDa heat shock protein, mitochondrial | 104 | 8 | 75 | 10,895/8.89 | 2.8e-07 | 6.65 |
| 9004 | P11517 | HBB2-RAT | Hemoglobin subunit beta-2 | 154 | 13 | 77 | 16,086/8.91 | 2.8e-12 | 95.65 |
| 9010 | P27364 | 3BHS5_RAT | 3 beta-hydroxysteroid dehydrogenase type 5 | 53 | 6 | 13 | 42,465/8.44 | 0.037 | [a] |
| 9001 | P11030 | ACBP_RAT | Acyl-CoA-binding protein | 61 | 6 | 43 | 10,021/8.78 | 0.0054 | 2.14 |
| Up-regulated proteins in the VPA-treated group | | | | | | | | | |
| 1007 | P11240 | COX5A_RAT | Cytochrome c oxidase subunit 5A, mitochondrial | 73 | 5 | 42 | 16,347/6.08 | 0.00034 | 2.31 |
| 8107 | Q63716 | PRDX1_RAT | Peroxiredoxin-1 | 86 | 6 | 33 | 22,323/8.27 | 1.8e-05 | [b] |
| 8303 | P04797 | G3P_RAT | Glyceraldehyde-3-phosphate dehydrogenase | 125 | 13 | 52 | 36,090/8.14 | 2.3e-09 | 2.7 |
| 8405 | P05065 | ALDOA_RAT | Fructose-bisphosphate aldolase A | 187 | 20 | 70 | 39,783/8.31 | 1.4e-15 | 2.3 |
| 6602 | P39950 | CCNG1_RAT | Cyclin-G1 | 59 | 5 | 26 | 33,912/9.09 | 0.0086 | 2 |
| 8005 | P10111 | PPIA_RAT | Peptidyl-prolyl *cis–trans* isomerase A | 126 | 17 | 76 | 18,091/8.34 | 1.8e-09 | [b] |
| 8021 | P10111 | PPIA_RAT | Peptidyl-prolyl *cis–trans* isomerase A | 121 | 12 | 68 | 18,091/8.34 | 5.7e-09 | 3.85 |

**Table 2** continued

| Spots number | Primary accession number | Protein ID | Protein name | Score | Peptides matched | Sequence coverage (%) | Theoretical Mr/PI | Expected | Fold change |
|---|---|---|---|---|---|---|---|---|---|
| 4517 | Q01986 | MP2K1_RAT | Dual specificity mitogen-activated protein kinase kinase 1 | 100 | 11 | 32 | 43,779/6.18 | 7.3e-07 | 2.14 |
| 4305 | O88989 | MDHC_RAT | Malate dehydrogenase, cytoplasmic | 148 | 13 | 38 | 36,631/6.16 | 1.1e-11 | 2.3 |
| 4314 | P16446 | PIPNA_RAT | Phosphatidylinositol transfer protein alpha isoform | 126 | 9 | 26 | 32,115/5.97 | 1.8e-09 | 2.14 |
| 4616 | P05370 | G6PD_RAT | Glucose-6-phosphate 1-dehydrogenase | 221 | 19 | 40 | 59,794/5.97 | 5.7e-19 | 2 |
| 3612 | Q5XIF6 | TBA4A_RAT | Tubulin alpha-4A chain | 94 | 13 | 45 | 50,634/4.95 | 3.1e-06 | 2.3 |
| 5708 | P09951 | SYN1_RAT | Synapsin-1 | 57 | 12 | 28 | 74,114/9.81 | 0.013 | 4.55 |
| 5813 | P21575 | DYN1_RAT | Dynamin-1 | 83 | 10 | 13 | 97,576/6.44 | 3.3e-05 | 2.18 |
| 5818 | P21575 | DYN1_RAT | Dynamin-1 | 122 | 19 | 22 | 97,576/6.44 | 4.5e-09 | 2.14 |
| 7101 | P23928 | CRYAB_RAT | Alpha-crystallin B chain | 81 | 7 | 45 | 20,076/6.76 | 5.3e-05 | 2.31 |

[a] Proteins expressed only in the epilepsy group compared with the VPA-treated group

[b] Proteins expressed only in the VPA-treated group compared with the epilepsy group

of several spots representing the same protein, probably reflecting splicing forms or posttranslational modifications, may explain the aberrant expression of the proteins.

Synaptic reorganization in the mossy fiber pathway results in translamellar hyperexcitability in the hippocampal formation. Neurophysiological studies demonstrate a correlation between the degree of cellular hyperexcitability of granule cells and the degree of synaptic reorganization of the mossy fiber pathway, a form of morphological plasticity observed in patients with MTLE and in experimental models of MTLE (Schwartzkroin 1986; Franck et al. 1995). To validate the results of 2-DE and to detect the protein expression levels that we screened in MTLE rat hippocampus, we used Western blot to measure the expression levels of synapse-related proteins synapsin-1, dynamin-1 and neurogranin in MTLE rat hippocampus. Furthermore, to evaluate if those three proteins were related to human MTLE pathogenesis or not, we detected their expression levels in MTLE human patient hippocampus. The protein levels were essentially coincidental with the proteome analysis. However, it was demonstrated that synapsin-1, dynamin-1 and neurogranin were closely related to the pathogenesis of human MTLE.

## Changed proteins in synaptic function and neurotransmitter release

A common feature of all AEDs is performing actions in synaptic transmission. Synapse properties probably play a critical role in the mechanism of MTLE. Synaptic reorganization of the mossy fiber pathway has received considerable attention over the past two decades. A potential mechanism of this reorganization is the increased excitability of the hippocampal network through the formation of new recurrent excitatory collaterals (Cavazos and Cross 2006). Reorganization of the epileptic circuitry with newly sprouted recurrent excitatory synapses has been considered as a putative mechanism explaining, at least in part, the cellular hyperexcitability observed in intractable MTLE. The impairment of the synaptic function leads to imbalance between excitation and inhibition in neural circuits. Characterization of synaptic protein complexes in rat brain can provide essential insights into the molecular mechanisms underlying epilepsy (Fukata et al. 2006). We screened three proteins closely associated with synaptic function in this study: synapsin-1, dynamin-1 and neurogranin.

Synapsin-1 is a synaptic vesicle-associated protein involved in the regulation of synaptogenesis and neurotransmitter release. It has also been proposed to play a role in the organization of cytoskeletal architecture in the presynaptic terminal (Fioravante et al. 2007). Synapsin-1 interacts with both lipid and protein components of synaptic vesicles

**Table 3** Identification of the differentially expressed proteins in rat hippocampus of the epilepsy group compared with the non-epilepsy group by MALDI-TOF–MS

| Spots number | Primary accession number | Protein ID | Protein name | Score | Peptides matched | Sequence coverage (%) | Theoretical Mr/PI | Expect | Fold change |
|---|---|---|---|---|---|---|---|---|---|
| Up-regulated proteins in the epilepsy group | | | | | | | | | |
| 4614 | P11598 | PDIA3_RAT | Protein disulfide-isomerase A3 | 246 | 26 | 50 | 57,044/5.88 | 1.8e-21 | 2.64 |
| 8010 | P07335 | KCRB_RAT | Creatine kinase B-type | 58 | 7 | 15 | 42,983/5.39 | 0.011 | 2.78 |
| 8106 | Q5XID9 | Q5XID9_RAT | Tusc4 protein | 81 | 9 | 22 | 51,404/8.48 | 0.00056 | 7.69 |
| 4008 | P02767 | TTHY_RAT | Transthyretin | 55 | 5 | 39 | 15,824/5.77 | 0.024 | 2.16 |
| 3005 | Q04940 | NEUG_RAT | Neurogranin | 82 | 5 | 43 | 7,720/6.54 | 4e-05 | 2.07 |
| 7202 | P27139 | CAH2_RAT | Carbonic anhydrase 2 | 105 | 6 | 35 | 29,267/6.89 | 2.3e-07 | 2.11 |
| 7108 | P39069 | KAD1_RAT | Adenylate kinase isoenzyme 1 | 164 | 14 | 68 | 21,684/7.66 | 2.8e-13 | 2.07 |
| 6415 | P43165 | CAH5A_RAT | Carbonic anhydrase 5A, mitochondrial | 52 | 6 | 23 | 34,477/8.48 | 0.044 | 5.88 |
| 5616 | O08651 | SERA_RAT | D-3-phosphoglycerate dehydrogenase | 101 | 10 | 28 | 57,256/6.28 | 5.7e-07 | 2.27 |
| 7109 | Q7M767 | UB2V2_RAT | Ubiquitin-conjugating enzyme E2 variant 2 | 66 | 5 | 45 | 16,399/7.79 | 0.0017 | 2.78 |
| 8114 | P45592 | COF1_RAT | Cofilin-1 | 82 | 10 | 67 | 18,749/8.22 | 5.1e-05 | [a] |
| 8103 | Q5I0D1 | GLOD4_RAT | Glyoxalase domain-containing protein 4 | 53 | 6 | 17 | 33,532/5.11 | 0.037 | 3.13 |
| 9002 | P10111 | PPIA_RAT | Peptidyl-prolyl *cis–trans* isomerase A | 131 | 11 | 68 | 18,091/8.34 | 5.7e-10 | [a] |
| 3502 | P47819 | GFAP_RAT | Glial fibrillary acidic protein delta | 99 | 19 | 37 | 49,984/5.35 | 2.3e-06 | 2.27 |
| 9011 | P56391 | CX6B1_MOUSE | Cytochrome c oxidase subunit VIb isoform 1 | 100 | 6 | 63 | 10,293/8.96 | 6.9e-06 | 2 |
| 9102 | Q63716 | PRDX1_RAT | Peroxiredoxin-1 | 117 | 14 | 71 | 22,323/8.27 | 1.4e-08 | [a] |
| 9004 | P11517 | HBB2_RAT | Hemoglobin subunit beta-2 | 154 | 13 | 77 | 16,086/8.91 | 2.8e-12 | 2.11 |
| 9003 | P01946 | HBA_RAT | Hemoglobin subunit alpha-1/2 | 109 | 6 | 50 | 15,490/7.82 | 9e-08 | 2.27 |
| 9005 | P26772 | CH10_RAT | 10 kDa heat shock protein, mitochondrial | 104 | 8 | 75 | 10,895/8.89 | 2.8e-07 | [a] |
| 8021 | P10111 | PPIA_RAT | Peptidyl-prolyl *cis–trans* isomerase A | 121 | 12 | 68 | 18,091/8.34 | 5.7e-09 | 7.29 |
| 9001 | P11030 | ACBP_RAT | Acyl-CoA-binding protein | 61 | 6 | 43 | 10,021/8.78 | 0.0054 | [a] |
| 5011 | P45592 | COF1_RAT | Cofilin-1 | 64 | 5 | 45 | 18,749/8.22 | 0.0029 | 2.31 |
| 2003 | P55051 | FABP7_RAT | Fatty acid-binding protein, brain | 92 | 7 | 69 | 15,140/5.46 | 4.5e-06 | [a] |
| Up-regulated proteins in the non-epilepsy group | | | | | | | | | |
| 5403 | Q561S0 | NDUAA_RAT | NADH dehydrogenase [ubiquinone] 1 alpha subcomplex subunit 10, mitochondrial | 144 | 11 | 65 | 40,753/7.64 | 4.5e-10 | 5.88 |
| 3501 | P07335 | KCRB_RAT | Creatine kinase B-type | 103 | 16 | 45 | 42,983/5.39 | 3.6e-07 | 3.12 |
| 3612 | Q5XIF6 | TBA4A_RAT | Tubulin alpha-4A chain | 94 | 13 | 45 | 50,634/4.95 | 3.1e-06 | 2.26 |
| 5206 | P97633 | KC1A_RAT | Casein kinase I isoform alpha | 62 | 7 | 33 | 37,699/9.55 | 0.019 | 2.19 |
| 5818 | P21575 | DYN1_RAT | Dynamin-1 | 122 | 19 | 22 | 97,576/6.44 | 4.5e-09 | 2.23 |
| 7404 | P13221 | AATC_RAT | Aspartate aminotransferase, cytoplasmic | 245 | 18 | 61 | 46,628/6.73 | 2.3e-21 | 6.58 |
| 7803 | Q9ER34 | ACON_RAT | Aconitate hydratase, mitochondrial | 230 | 25 | 35 | 86,121/7.87 | 2.8e-18 | 2.26 |
| 6602 | P39950 | CCNG1_RAT | Cyclin-G1 | 59 | 5 | 26 | 33,912/9.09 | 0.0086 | 5.56 |

**Table 3** continued

| Spots number | Primary accession number | Protein ID | Protein name | Score | Peptides matched | Sequence coverage (%) | Theoretical Mr/PI | Expect | Fold change |
|---|---|---|---|---|---|---|---|---|---|
| 4517 | Q01986 | MP2K1_RAT | Dual specificity mitogen-activated protein kinase kinase 1 | 100 | 11 | 32 | 43,779/6.18 | 7.3e-07 | 5.56 |
| 4609 | P85108 | TBB2A_RAT | Tubulin beta-2A chain | 147 | 14 | 36 | 50,274/4.78 | 1.4e-11 | 3.31 |
| 5305 | O35077 | GPDA_RAT | Glycerol-3-phosphate dehydrogenase [$NAD^+$], cytoplasmic | 82 | 6 | 26 | 38,112/6.16 | 4.9e-05 | 2.39 |
| 5315 | P85972 | VINC_RAT | Vinculin | 57 | 15 | 16 | 11,7112/5.83 | 0.014 | 2.18 |
| 5708 | P09951 | SYN1_RAT | Synapsin-1 | 57 | 12 | 28 | 74,114/9.81 | 0.013 | 50 |
| 5813 | P21575 | DYN1_RAT | Dynamin-1 | 83 | 10 | 13 | 97,576/6.44 | 3.3e-05 | 2.87 |
| 4618 | Q91ZN1 | COR1A_RAT | Coronin-1A | 193 | 14 | 45 | 51,717/6.05 | 3.6e-16 | 2.18 |
| 5719 | O35814 | STIP1_RAT | Stress-induced-phosphoprotein 1 | 131 | 22 | 45 | 63,158/6.40 | 5.7e-10 | 2.07 |
| 6421 | Q6DGG0 | PPID_RAT | 40 kDa peptidyl-prolyl *cis–trans* isomerase | 106 | 16 | 55 | 40,740/6.73 | 1.8e-07 | 2.39 |
| 1103 | P63029 | TCTP_RAT | Translationally-controlled tumor protein | 80 | 6 | 33 | 19,564/4.76 | 6.9e-05 | 2.14 |
| 5414 | Q5RJQ4 | SIRT2_RAT | NAD-dependent deacetylase sirtuin-2 | 110 | 11 | 36 | 39,921/6.67 | 7.1e-08 | 2.18 |
| 4305 | O88989 | MDHC_RAT | Malate dehydrogenase, cytoplasmic | 148 | 13 | 38 | 36,631/6.16 | 1.1e-11 | 3.31 |
| 4314 | P16446 | PIPNA_RAT | Phosphatidylinositol transfer protein alpha isoform | 126 | 9 | 26 | 32,115/5.97 | 1.8e-09 | 2.87 |
| 4616 | P05370 | G6PD_RAT | Glucose-6-phosphate 1-dehydrogenase | 221 | 19 | 40 | 59,794/5.97 | 5.7e-19 | 3.11 |
| 5709 | Q6P502 | TCPG_RAT | T-complex protein 1 subunit gamma | 142 | 13 | 33 | 61,179/6.23 | 4.5e-11 | 53.93 |
| 6210 | P11348 | DHPR_RAT | Dihydropteridine reductase | 175 | 14 | 59 | 25,764/7.67 | 2.3e-14 | [b] |
| 7101 | P23928 | CRYAB_RAT | Alpha-crystallin B chain | 81 | 7 | 45 | 20,076/6.76 | 5.3e-05 | [b] |

[a] Proteins expressed only in the epilepsy group compared with the non-epilepsy group

[b] Proteins expressed only in the non-epilepsy group compared with the epilepsy group

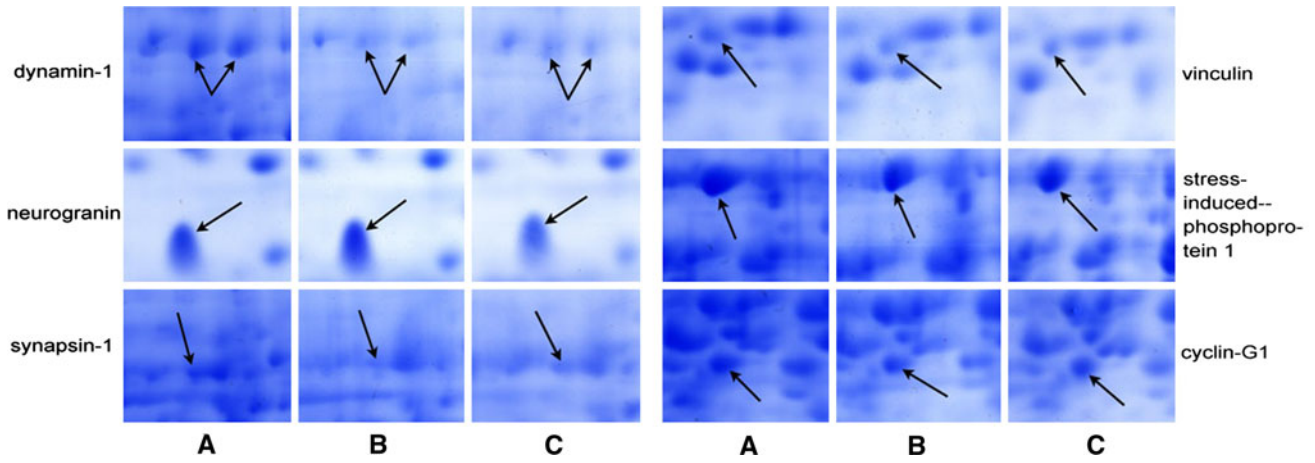


**Fig. 4** 2-DE gel images of six selected proteins are indicated by *arrows* in the panels. Each panel shows an *enlarged view* of the gel spots in Fig. 3 and is ranked from left to right. **a** Non-epilepsy group, **b** epilepsy group, **c** VPA-treated group

and with cytoskeletal proteins. Phosphorylation modulates interactions of synapsin-1 with both synaptic vesicles and cytoskeletal components. It acts as a phosphorylation state-dependent regulator of synaptic vesicle mobilization and neurotransmitter release (Hilfiker et al. 2005). In electroconvulsive treatment rats, phosphorylation of synapsin-1 at multiple sites was decreased during brief seizure activity in hippocampal and parieto-cortical homogenates (Yamagata 2003). Deletion of the synapsin-1 genes in mice causes late onset epileptic seizures and enhanced experimental temporal lobe epilepsy (Terada et al. 1999). In our study, we observed that synapsin-1 was down-regulated remarkably in the epilepsy group, which was revived partly after VPA ministration. It was suggested that synapsin-1 was involved in the pathogenesis of MTLE by regulating synaptogenesis and neurotransmitter release, and that VPA interfered with the actions of synapsin-1 to prevent the occurrence of seizures.

Dynamin-1 concentrates in the presynapse and plays an essential role in vesicle formation and synaptic transmission. It is a GTP-hydrolyzing protein and a key element in the clathrin-mediated endocytosis of secretory granules and neurovesicles at the plasma membrane (Evergren et al. 2004). In vivo, profilins co-localize with dynamin-1 and synapsin in axonal and dendritic processes (Witke et al. 1998). The GTPase dynamin-1 represents a potentially highly efficacious target that indirectly modulates neurotransmitter loading, leading to reduced epileptic synaptic transmission while limiting potential side effects. The critical role of dynamin-1 in vesicle formation and synaptic transmission makes it a novel target of AEDs. In our study, dynamin-1 was remarkably down-regulated in VPA-treated rats compared with epilepsy and non-epilepsy rats. Additionally, Western blot found that its regulation was lower in the hippocampus of MTLE patients. While the causes of this change are unclear, it may involve the alteration of vesicle formation and/or synaptic transmission.

Neurogranin is a brain-specific protein expressed in the hippocampus that accumulates postsynaptically in the dendritic spines of neurons. It has been implicated in the modulation of postsynaptic signal transduction pathways and synaptic plasticity (Kubota et al. 2008). Neurogranin binds calmodulin (CaM), and its binding affinity is reduced by increasing $Ca^{2+}$, phosphorylation by PKC or oxidation by oxidants. Neurogranin enhances long-term potentiation and learning by promoting calcium-mediated signaling (Huang et al. 2004). Neurogranin may be linked to neurite formation by affecting the expression of several microtubule-related proteins (Gao et al. 2008). Liu (Liu et al. 2008) found that neurogranin had a differential expression in MTLE rats. In our experiment, neurogranin was up-regulated in both MTLE rats and MTLE patient hippocampus. It is hypothesized that it participates in the pathogenesis of MTLE and the action of VPA by altering interactions with CaM, phosphatidic acid and alpha-tubulin, producing changes in postsynaptic signal transduction and synaptic plasticity.

Taken together, both synapsin-1 and dynamin-1 have functions in the presynaptic membrane, while neurogranin plays a role in the postsynaptic membrane. As synapse has a close relationship with epilepsy's mechanism and is a most important target of many AEDs, the synaptic-related proteins synapsin-1, dynamin-1 and neurogranin probably play a critical role in MTLE's mechanism and VPA's efficacy. Moreover, all three of these proteins share a close relationship with cytoskeletal proteins, which will be discussed below. Based on the many cytoskeletal proteins and synaptic relative proteins that we have found differentially expressed in this study, we hypothesized that cytoskeleton and synapse are critical collaborators in MTLE.

**Table 4** Global analysis of the differentially expressed proteins

| Spots number | Primary accession number | Protein name | Function |
|---|---|---|---|
| Proteins always up-regulated in the epilepsy group versus non-epilepsy and VPA-treated groups | | | |
| 3005 | Q04940 | Neurogranin | Synaptic plasticity, spatial learning, |
| 4008 | P02767 | Transthyretin | Thyroid hormone-binding protein |
| 4614 | P11598 | Protein disulfide-isomerase A3 | Isomerase activity |
| 7109 | Q7M767 | Ubiquitin-conjugating enzyme E2 variant 2 | DNA repair |
| 8010 | P07335 | Creatine kinase B-type | Transferase activity, energy transduction |
| 8114 & 5011 | P45592 | Cofilin-1 | Actin polymerization and depolymerization |
| 9011 | P56391 | Cytochrome c oxidase subunit VIb isoform 1 | Transporter activity, oxidoreductase activity |
| 6415 | P43165 | Carbonic anhydrase 5A, mitochondrial | Lyase activity |
| 7202 | P27139 | Carbonic anhydrase 2 | Lyase activity |
| 7108 | P39069 | Adenylate kinase isoenzyme 1 | Energy metabolism, nucleotide synthesis |
| 9102 | Q63716 | Peroxiredoxin-1 | Antioxidant activity, oxidoreductase activity |
| 9002 | P10111 | Peptidyl-prolyl *cis–trans* isomerase A | Isomerase activity |
| 9003 | P01946 | Hemoglobin subunit alpha-1/2 | Oxygen binding, transporter activity |
| 9005 | P26772 | 10 kDa heat shock protein, mitochondrial | Mitochondrial protein biogenesis, suppresses the ATPase activity |
| 9004 | P11517 | Hemoglobin subunit beta-2 | Oxygen binding, transporter activity |
| 9001 | P11030 | Acyl-CoA-binding protein | Intracellular carrier of acyl-CoA esters, modulating the action of the GABA receptor |
| Proteins up-regulated over twofold after VPA administration, which down-regulated in the epilepsy compared with the non-epilepsy group | | | |
| 3612 | Q5XIF6 | Tubulin alpha-4A chain | Regulating the assembly and dynamics of axonemal microtubules |
| 5818 & 5813 | P21575 | Dynamin-1 | Vesicular trafficking processes, receptor-mediated endocytosis |
| 7101 | P23928 | Alpha-crystallin B chain | Structural molecule activity |
| 6602 | P39950 | Cyclin-G1 | Growth regulation |
| 4517 | Q01986 | Dual specificity mitogen-activated protein kinase kinase 1 | Activates ERK1 and ERK2 MAP kinases |
| 5708 | P09951 | Synapsin-1 | Coating synaptic vesicles, binds to the cytoskeleton, regulating neurotransmitter release |
| 4305 | O88989 | Malate dehydrogenase, cytoplasmic | Antioxidant activity, catalytic activity |
| 4314 | P16446 | Phosphatidylinositol transfer protein alpha isoform | Transporter activity, catalytic activity |
| 4616 | P05370 | Glucose-6-phosphate 1-dehydrogenase | Oxidoreductase activity, catalytic activity |

## Changed proteins with cytoskeletal structure and dynamics

The cytoskeleton is a highly dynamic structure that not only forms the scaffold, the basis of cell morphology and plasticity, but also plays a major role in transport and signalling (Yang et al. 2006). It comprises three major types of cytoplasmic structural proteins: microtubules, actin and intermediate filaments. Derangement of several structures of the brain's cytoskeleton has been reported in different forms of neurodegenerative disease and may reflect or lead to neuropathological changes such as neuronal death and synaptosomal loss (Yang et al. 2006; Shim and Lubec 2002; Weitzdoerfer et al. 2002). This study identified several differentially expressed proteins involved in cytoskeletal structure and dynamics, including cofilin-1, tubulin alpha-4A chain, tubulin beta-2A chain, coronin-1A, glial fibrillary acidic protein and NAD-dependent deacetylase sirtuin-2 (SIR2-like).

Cofilin-1, a regulatory molecule of actin filaments (F-actin), can depolymerise F-actin, leading to structural or functional changes in spines in response to normal physiological activity (Ouyang et al. 2007). In this study, cofilin-1 was always up-regulated in the epilepsy group, independent of VPA treatment. Therefore, cofilin-1 may be a key element in the pathogenesis of MTLE and its drug

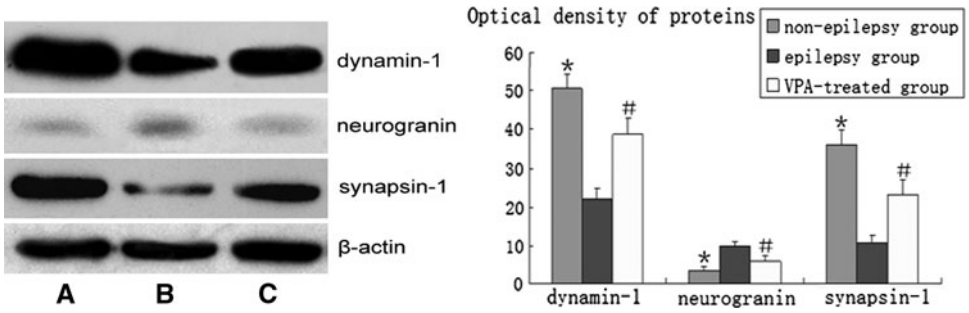


**Fig. 5** Western blot analysis to validate the differential expression for dynamin-1, synapsin-1 and neurogranin in the three rat groups. The total proteins (30 μg/lane) extracted from rat hippocampus was separated by SDS-PAGE for each sample and probed with the primary antibody. Densitometry analysis was performed using FluorChem software. *Left* a representative Western blot visualizing dynamin-1, synapsin-1 and neurogranin expression levels. *Right* band density was digitized. Significant differences are indicated: $^{*}p < 0.01$, non-epilepsy group versus epilepsy group; $^{\#}p < 0.01$, VPA-treated group versus epilepsy group. **a** non-epilepsy group, **b** epilepsy group, **c** VPA-treated group

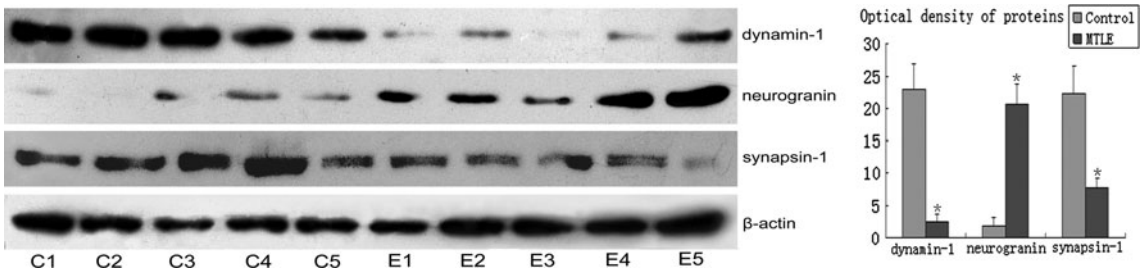


**Fig. 6** Western blot analysis of dynamin-1, synapsin-1 and neurogranin in the hippocampus of controls and patients with MTLE to further validate the reliability of the differentially expressed proteins we obtained. Total proteins (30 μg/lane) extracted from the human hippocampus were separated by SDS-PAGE for each sample and probed with the primary antibody. Densitometry analysis was performed using FluorChem software. *Left* a representative Western blot visualizing dynamin-1, synapsin-1 and neurogranin expression levels. *Right* band density was digitized. In comparison with controls, the level of significance was considered at $^{*}p < 0.01$. C1–C5 represented five patients without brain disease and E1–E5 represented five patients with MTLE

resistance. But we need more experimental support, as outlined in the following investigations.

The coronin-1 protein is a member of the coronin family of actin-binding proteins, which is selectively expressed in immune cells and has been suggested to play crucial roles in leukocyte functions, including cell migration and phagocytosis. The phosphorylation of coronin-1 down-regulates its association with actin and modulates the reorganization of actin-containing cytoskeleton (Oku et al. 2008). We found that coronin-1 was down-regulated in the epilepsy group.

SIR2-like is an NAD-dependent deacetylase that is co-localized with microtubules and is a key element in DNA repair and recombination, microtubule organization and control of cell cycles (Dryden et al. 2003). Decreased levels may explain multiple expressional differences observed in MTLE such as neuronal death and impaired DNA repair. Deficient SIR2-like in MTLE furthermore fits or maybe even generates cytoskeletal deterioration, as this protein is known to specifically deacetylate tubulin (North et al. 2003). In the present study, the down-regulation of SIR2-like observed in the epilepsy group compared with the VPA-treated group suggests that SIR2-like may contribute to the genesis of pharmacoresistant MTLE.

There were many cytoskeletal and relative proteins we screened that were differentially expressed in this study. They are able to interrelate with synaptic proteins, neurotransmitter receptors, cell junction proteins, molecular chaperones, signal molecules and so on, playing key roles by integrating different types of life functions.

## Changed proteins in cell junctions

We found that the cell junction protein vinculin was differentially expressed in this study. Vinculin is a highly conserved intracellular protein with a crucial role in the maintenance and regulation of cell adhesion and migration. On recruitment to cell–cell and cell–matrix adherens-type junctions, vinculin becomes activated and mediates various protein–protein interactions that regulate the links between F-actin and the cadherin and integrin families of cell adhesion molecules (Bakolitsa et al. 2004). Here, vinculin was found among the down-regulated proteins in the epilepsy group and up-regulated over twofolds after VPA

administration. Therefore, it may play a role in VPA's protective effects. Further studies are warranted to determine whether or not there are changes in gap junctions leading to abnormalities in ions and neurotransmitters in seizure attacks.

### Changed proteins in energy metabolism and mitochondrial function

We screened a series of differentially expressed proteins related to energy metabolism and mitochondrial function, including peroxiredoxin-1, cytochrome c oxidase subunit VIb isoform 1, cytochrome c oxidase subunit 5A, creatine kinase, creatine kinase B-type, glyoxalase domain-containing protein 4, 60 kDa heat shock protein, 10 kDa heat shock protein, carbonic anhydrase 5A, fructose-bisphosphate aldolase A, aconitate hydratase, 3 beta-hydroxysteroid dehydrogenase type 5, 40 kDa peptidyl-prolyl *cis–trans* isomerase, NADH dehydrogenase 1 alpha subcomplex subunit 10, glucose-6-phosphate 1-dehydrogenase, malate dehydrogenase, and cytoplasmic and glycerol-3-phosphate dehydrogenase.

The antioxidant protein peroxiredoxin-1 is a thioredoxin peroxidase that is involved in the regulation of proliferation and differentiation of mammalian cells. We observed that peroxiredoxin-1 was always up-regulated in the epilepsy group. Mitochondria-specific peroxidases (peroxiredoxins) are suggested to regulate cytochrome c release from mitochondria, which is a critical early step in the apoptotis-signaling pathway (Ueda et al. 2002). In this study, we observed a series of proteins related to the apoptotis-signaling pathway, including cytochrome c oxidase subunit VIb isoform 1, cytochrome c oxidase subunit 5A and many of the enzymes that regulate energy metabolism. All of these findings suggest that an imbalance of energy metabolism and mitochondrial function are involved in the development of MTLE and its response to VPA.

### Changed proteins in molecular chaperones

The involvement of chaperones in the process of neurodegenerative disorders, including epilepsies, has been previously reported (Yoo et al. 2001). The chaperones the levels of which changed in our study were T-complex protein 1 (TCP-1), alpha B-crystallin and heat shock proteins (HSPs). HSPs play a central role in the cellular mechanisms of stress tolerance. We found two mitochondrial related HSPs in our study: 60 and 10 kDa heat shock proteins.

TCP-1 is the major candidate for chaperoning cytoskeleton elements specific to tubulin (Schuller et al. 2001). Impairment of chaperones may well be responsible for the development of cytoskeletal deficit, but may also be only a by-product, as status epilepticus is followed by overexpression of several heat shock components (Little et al. 1996).

Alpha B-crystallin, a small chaperone protein that binds to unfolded proteins and inhibits aggregation, is important for cell survival and genomic stability and associates with the tubulin cytoskeleton (Xi et al. 2006). It plays a cytoprotective function, preventing neuron death and delaying disease progression (Lee et al. 2005). The increase in expression of alpha B-crystallin after VPA treatment might play a role in the neuroprotective effect.

### Changed proteins in signal regulation and others

Dual specificity mitogen-activated protein kinase kinase 1 (MAPKK1), a substrate of MAP kinase kinases, may contribute to cytoskeletal alteration by impairing phosphorylation of cytoskeleton proteins, proteins known to be substrates of MAP kinase kinases (Horne and Guadagno 2003). MAPKK also shows a link to synaptic function (Hoeffer et al. 2003), and the observed decrease of MAPKK1 in the epilepsy group may partially help to explain the synaptosomal deficit in MTLE.

Stress-induced phosphoprotein 1 mediates the association of the molecular chaperones (Demand et al. 1998). It down-regulated in the epilepsy group and up-regulated after VPA administration, suggesting that stress-induced-phosphoprotein 1 functions in VPA's anti-epilepsy effects.

## Conclusion

Our study showed aberrant expression of proteins in synaptic and neurotransmitter release function, cytoskeletal structure and dynamics, cell junctions, energy metabolism and mitochondrial function, molecular chaperones, signal regulation, etc., in the hippocampus of non-spontaneous seizure rats, spontaneous seizure rats and rats that were administered VPA. Parts of the screened proteins we examined also had differential expression in the MTLE human patient hippocampus. These findings demonstrate the significance of abnormal expression of structural proteins in hippocampal lesions, mitochondrial proteins in apoptosis and synaptic transmission, memory formation and plasticity, when elucidating the physiological and pathophysiological properties of MTLE and its pharmacological mechanism after AEDs.

Based on a chronic MTLE animal model where disease is induced in developing rats, our data directly support the idea that abnormal protein–protein networks play an important role in the development of MTLE and are involved in abnormal brain plasticity formation. Meanwhile, early intervention with VPA at the onset of

spontaneous seizures could achieve seizure freedom in MTLE models with an identified optimum medication intervention time. The differentially expressed proteins between VPA-treated and untreated rats provided important clues to explore new biomarkers for the development of pharmacological therapies targeted at MTLE.

**Acknowledgments** We thank Dr. Zhiquan Yang (Department of Neurosurgery, Xiangya Hospital, China) for providing the experimental hippocampus of MTLE patients and Dr. Zhaojun Duan (Department of Clinical Laboratory, Xiangya Hospital, China) for critically reviewing the manuscript. This work was supported by the National Natural Science Foundation of China, 30901631. The authors declare that there is no conflict of interest in either financial support or relationships.

## References

Babb TL, Kupfer WR, Pretorius JK, Crandall PH, Levesque MF (1991) Synaptic reorganization by mossy fibers in human epileptic fascia dentata. Neuroscience 42(2):351–363

Bakolitsa C, Cohen DM, Bankston LA, Bobkov AA, Cadwell GW, Jennings L, Critchley DR, Craig SW, Liddington RC (2004) Structural basis for vinculin activation at sites of cell adhesion. Nature 430(6999):513–515

Cavazos JE, Cross DJ (2006) The role of synaptic reorganization in mesial temporal lobe epilepsy. Epilepsy Behav 8(3):483–493

Danzer SC, He X, Loepke AW, McNamara JO (2010) Structural plasticity of dentate granule cell mossy fibers during the development of limbic epilepsy. Hippocampus 20(1):113–124

Demand J, Luders J, Hoehfeld J (1998) The carboxy-terminal domain of Hsc70 provides binding sites for a distinct set of chaperone cofactors. Mol Cell Biol 18(4):2023–2028

Dryden SC, Nahhas FA, Nowak JE, Goustin AS, Tainsky MA (2003) Role for human SIRT2 NAD-dependent deacetylase activity in control of mitotic exit in the cell cycle. Mol Cell Biol 23(9):3173–3185

Engel J Jr (1996) Introduction to temporal lobe epilepsy. J Epilepsy Res 26(1):141–150

Evergren E, Tomilin N, Vasylieva E, Sergeeva V, Bloom O, Gad H, Capani F, Shupliakov O (2004) A pre-embedding immunogold approach for detection of synaptic endocytic proteins in situ. J Neurosci Methods 135(1–2):169–174

Fioravante D, Liu RY, Netek AK, Cleary LJ, Byrne JH (2007) Synapsin regulates basal synaptic strength, synaptic depression, and serotonin-induced facilitation of sensorimotor synapses in Aplysia. J Neurophysiol 98(6):3568–3580

Franck JE, Pokorny J, Kunkel DD, Schwartzkroin PA (1995) Physiologic and morphologic characteristics of granule cell circuitry in human epileptic hippocampus. Epilepsia 36(6):543–558

Fukata Y, Adesnik H, Iwanaga T, Bredt DS, Nicoll RA, Fukata M (2006) Epilepsy-related ligand/receptor complex LGI1 and ADAM22 regulate synaptic transmission. Science 313(5794): 1792–1795

Gao Y, Tatavarty V, Korza G, Levin MK, Carson JH (2008) Multiplexed dendritic targeting of alpha calcium calmodulin-dependent protein kinase II, neurogranin, and activity-regulated cytoskeleton-associated protein RNAs by the A2 pathway. Mol Biol Cell 19(5):2311–2327

Gluck MR, Jayatilleke E, Shaw S, Rowan AJ, Haroutunian V (2000) CNS oxidative stress associated with the kainic acid rodent model of experimental epilepsy. Epilepsy Res 39(1):63–71

Graves TD (2006) Ion channels and epilepsy. QJM 99(4):201–217

Greene ND, Bamidele A, Choy M, de Castro SC, Wait R, Leung KY, Begum S, Gadian DG, Scott RC, Lythgoe MF (2007) Proteome changes associated with hippocampal MRI abnormalities in the lithium pilocarpine-induced model of convulsive status epilepticus. Proteomics 7(8):1336–1344

Hamani C, Paulo I, Mello LE (2005) Neo-Timm staining in the thalamus of chronically epileptic rats. Braz J Med Biol Res 38(11):1677–1682

Hilfiker S, Benfenati F, Doussau F, Nairn AC, Czernik AJ, Augustine GJ, Greengard P (2005) Structural domains involved in the regulation of transmitter release by synapsins. J Neurosci 25(10):2658–2669

Hoeffer CA, Sanyal S, Ramaswami M (2003) Acute induction of conserved synaptic signaling pathways in *Drosophila melanogaster*. J Neurosci 23(15):6362–6372

Horne MM, Guadagno TM (2003) A requirement for MAP kinase in the assembly and maintenance of the mitotic spindle. J Cell Biol 161(6):1021–1028

Huang KP, Huang FL, Ger JT, Li J, Reymann KG, Balschun D (2004) Neurogranin/RC3 enhances long-term potentiation and learning by promoting calcium-mediated signaling. J Neurosci 24(47):10660–10669

Jabs R, Seifert G, Steinh user C (2008) Astrocytic function and its alteration in the epileptic brain. Epilepsia 49(2):3–12

Johannessen CU, Petersen D, Fonnum F, Hassel B (2001) The acute effect of valproate on cerebral energy metabolism in mice. Epilepsy Res 47(3):247–256

Kapur J (2008) Is epilepsy a disease of synaptic transmission? Epilepsy Curr 8(5):139–141

Kubota Y, Putkey JA, Shouval HZ, Waxham MN (2008) IQ-motif proteins influence intracellular free $Ca^{2+}$ in hippocampal neurons through their interactions with calmodulin. J Neurophysiol 99(1):264–276

Kwan P, Brodie MJ (2000) Epilepsy after the first drug fails: substitution or add-on? Seizure 9(7):464–468

Landmark CJ (2007) Targets for antiepileptic drugs in the synapse. Med Sci Monit 13(1):RA1–RA7

Lee S, Carson K, Rice-Ficht A, Good T (2005) Hsp20, a novel alpha-crystallin, prevents Abeta fibril formation and toxicity. Protein Sci 14(3):593–601

Leite JP, Cavalheiro EA (1995) Effects of conventional antiepileptic drugs in a model of spontaneous recurrent seizures in rats. Epilepsy Res 20(2):93–104

Little E, Tocco G, Baudry M, Lee AS, Schreiber SS (1996) Induction of glucose-regulated protein (glucose-regulated protein 78/BiP and glucose-regulated protein 94) and heat shock protein 70 transcripts in the immature rat brain following status epilepticus. Neuroscience 75(1):209–219

Liu XY, Yang JL, Chen LJ, Zhang Y, Yang ML, Wu YY, Li FQ, Tang MH, Liang SF, Wei YQ (2008) Comparative proteomics and correlated signaling network of rat hippocampus in the pilocarpine model of temporal lobe epilepsy. Proteomics 8(3):582–603

Lopantsev V, Both M, Draguhn A (2009) Rapid plasticity at inhibitory and excitatory synapses in the hippocampus induced by ictal epileptiform discharges. Eur J Neurosci 29(6):1153–1164

Mathern GW, Babb TL, Micevych PE, Blanco CE, Pretorius JK (1997) Granule cell mRNA levels for BDNF, NGF, and NT-3 correlate with neuron losses or supragranular mossy fiber sprouting in the chronically damaged and epileptic human hippocampus. Mol Chem Neuropathol 30(1–2):53–76

McPherson PS, Czernik AJ, Chilcote TJ, Onofri F, Benfenati F, Greengard P, Schlessinger J, De Camilli P (1994) Interaction of Grb2 via its Src homology 3 domains with synaptic proteins

including synapsin I. Proc Natl Acad Sci U S A 91(14):6486–6490

Moshe SL (1993) Seizures in the developing brain [J]. Neurology 43(11 Suppl 5):S3–S7

Muramatsu R, Ikegaya Y, Matsuki N et al (2008) Early-life status epilepticus induces ectopic granule cells in adult mice dentate gyrus [J]. Exp Neurol 211(2):503–510

North BJ, Marshall BL, Borra MT, Denu JM, Verdin E (2003) The human Sir2 ortholog, SIRT2, is an NADþ-dependent tubulin deacetylase. Mol Cell 11(2):437–444

Oku T, Kaneko Y, Murofushi K, Seyama Y, Toyoshima S, Tsuji T (2008) Phorbol ester-dependent phosphorylation regulates the association of p57/coronin-1 with the actin cytoskeleton. J Biol Chem 283(43):28918–28925

Ouyang Y, Yang XF, Hu XY, Erbayat-Altay E, Zeng LH, Lee JM, Wong M (2007) Hippocampal seizures cause depolymerization of filamentous actin in neurons independent of acute morphological changes. Brain Res 1143:238–246

Sarac S, Afzal S, Broholm H, Madsen FF, Ploug T, Laursen H (2009) EAAT-1 and EAAT-2 in temporal lobe and hippocampus in intractable temporal lobe epilepsy. APMIS 117(4):291–301

Schuller E, Gulesserian T, Seidl R, Cairns N, Lubec G (2001) Brain t-complex polypeptide 1 (TCP-1) related to its natural substrate beta1 tubulin is decreased in Alzheimer's disease. Life Sci 69(3):263–270

Schwartzkroin PA (1986) Hippocampal slices in experimental and human epilepsy. Adv Neurol 44:991–1010

Shim KS, Lubec G (2002) Drebrin, a dendritic spine protein, is manifold decreased in brains of patients with Alzheimer's disease and Down syndrome. Neurosci Lett 324(3):209–212

Terada S, Tsujimoto T, Takei Y, Takahashi T, Hirokawa N (1999) Impairment of inhibitory synaptic transmission in mice lacking synapsin I. J Cell Biol 145(5):1039–1048

Timofeev I, Bazhenov M, Avramescu S, Nita DA (2009) Posttraumatic epilepsy: the roles of synaptic plasticity. Neuroscientist (Epub ahead of print)

Ueda S, Masutani H, Nakamura H, Tanaka T, Ueno M, Yodoi J (2002) Redox control of cell death. Antioxid Redox Signal 4(3):405–414

Weitzdoerfer R, Fountoulakis M, Lubec G (2002) Reduction of actin-related protein complex in fetal Down syndrome brain. Biochem Biophys Res Commun 293(2):836–841

Williams PA, Dou P, Dudek FE (2004) Epilepsy and synaptic reorganization in a perinatal rat model of hypoxia–ischemia. Epilepsia 45(10):1210–1218

Witke W, Podtelejnikov AV, Di Nardo A, Sutherland JD, Gurniak CB, Dotti C, Mann M (1998) In mouse brain profilin I and profilin II associate with regulators of the endocytic pathway and actin assembly. EMBO J 17(4):967–976

Wong M (2008) Stabilizing dendritic structure as a novel therapeutic approach for epilepsy. Expert Rev Neurother 8(6):907–915

Wu LW, Peng J, Wei CP, Yin F (2009) Preliminary explorations of differentially expressed proteins in hippocampus of MTLE rats following treatment with valproate, some findings from comparative proteomics. 13th Asian Pacific Congress of Pediatrics. Shanghai. OR710

Xi JH, Bai F, McGaha R, Andley UP (2006) Alpha-crystallin expression affects microtubule assembly and prevents their aggregation. FASEB J 20(7):846–857

Yamagata Y (2003) New aspects of neurotransmitter release and exocytosis: dynamic and differential regulation of synapsin I phosphorylation by acute neuronal excitation in vivo. J Pharmacol Sci 93:22–29

Yang JW, Czech T, Felizardio M, Baumgartner C, Lubec G (2006) Aberrant expression of cytoskeleton proteins in hippocampus from patients with mesial temporal lobe epilepsy. Amino Acids 30(4):477–493

Yoo BC, Vlkolinsky R, Engidawork E, Cairns N, Fountoulakis M, Lubec G (2001) Differential expression of molecular chaperones in brain of patients with Down syndrome. Electrophoresis 22(6):1233–1241